Title:

SPECIFIC PREFERENCES IN LINEAGE CHOICE AND PHENOTYPIC PLASTICITY OF GLIOMA STEM CELLS UNDER BMP4 AND NOGGIN INFLUENCE

Guillermo Agustín Videla Richardson (1) willyvidelar@hotmail.com (5411) 5777-3200 ext. 7305
Carolina Paola Garcia (1) carolinapaolagarcia@gmail.com (5411) 5777-3200 ext. 7305
Alejandro Roisman (4) alejandroroisman@hotmail.com (5411) 4805-8803 ext. 241 FAX: (5411) 4803-9475
Irma Slavutsky (4) islavutsky@hematologia.anm.edu.ar (5411) 4805-8803 ext. 241 FAX: (5411) 4803-9475
Damián Darío Fernandez Espinosa (1) dfernandez@fleni.org.ar (5411) 5777-3200 ext. 7322
Leonardo Romorini (1) lromorini@fleni.org.ar (5411) 5777-3200 ext. 7315
Santiago Gabriel Miriuka (1) smiriuka@fleni.org.ar (5411) 5777-3200 ext. 7319
Naomi Arakaki (2) narakaki@fleni.org.ar (5411) 5777-3200 ext. 2320
Horacio Martinetto (3) hmartinetto@fleni.org.ar (5411) 5777-3200 ext. 1927
María Elida Scassa (1) mescassa@fleni.org.ar (5411) 5777-3200 ext. 7302
Gustavo Emilio Sevlever (2) gsevlever@fleni.org.ar (5411) 5777-3200 ext. 2326 FAX: (5411) 5777-3209

(1) Laboratorio de Investigación aplicada a Neurociencias (LIAN). Fundación para la Lucha contra las Enfermedades Neurológicas de la Infancia (FLENI). Ruta 9, Km 52.5, B1625XAF. Escobar. Provincia de Buenos Aires, Argentina.

(2) Laboratorio de Neuropatología, Departamento de Neuropatología y Biología Molecular. Fundación para la Lucha contra las Enfermedades Neurológicas de la Infancia (FLENI). Montañeses 2325, C1428AQK. Buenos Aires, Argentina.

(3) Laboratorio de Biología Molecular, Departamento de Neuropatología y Biología Molecular. Fundación para la Lucha contra las Enfermedades Neurológicas de la Infancia (FLENI). Montañeses 2325, C1428AQK. Buenos Aires, Argentina.

(4) Laboratorio de Genética de Neoplasias Linfoides, Instituto de Medicina Experimental, CONICET. Academia Nacional de Medicina. J.A. Pacheco de Melo 3081, C1425AUM. Buenos Aires, Argentina.

This article has been accepted for publication and undergone full peer review but has not been through the copyediting, typesetting, pagination and proofreading process, which may lead to differences between this version and the Version of Record. Please cite this article as doi: 10.1111/bpa.12263

Abstract

Although BMP4-induced differentiation of glioma stem cells is well recognized, details of the cellular responses triggered by this morphogen are still poorly defined. In this study we established several glioma stem cell-enriched cell lines (GSC-ECLs) from high grade gliomas. The expansion of these cells as adherent monolayers, and not as floating neurospheres, enabled a thorough study of the phenotypic changes that occurred during their differentiation. Herein, we evaluated GSC-ECLs behavior towards differentiating conditions by depriving them of growth factors and/or by adding BMP4 at different concentrations. After analyzing cellular morphology, proliferation and lineage marker expression we determined that GSC-ECLs have distinct preferences in lineage choice, where some of them showed an astrocyte fate commitment and others a neuronal one. We found that this election seems to be dictated by the expression pattern of BMP signaling components present in each GSC-ECL. Additionally, treatment of GSC-ECLs with the BMP antagonist Noggin also led to evident phenotypic changes. Interestingly, under certain conditions some GSC-ECLs adopted an unexpected smooth muscle-like phenotype. As a whole, our findings illustrate the wide differentiation potential of glioma stem cells, highlighting their molecular complexity and paving a way to facilitate personalized differentiating therapies.

Key words: cancer stem cells; multipotency; differentiation; glioblastoma; BMP4; Noggin

Introduction

Gliomas are the most frequent primary brain tumors in adults (13). They are classified as astrocytoma, oligodendroglioma, or ependymoma, based on the glial cell type that predominates in the tumor (28). Among gliomas, glioblastoma multiforme (GBM) is a diffusely and rapidly growing tumor with distinctive histological features. Despite aggressive multimodal therapies consisting of surgical resection, radiotherapy, and chemotherapy, the median survival in GBM is less than 15 months (48). Although their cell heterogeneity is well described, the initial malignant transformation events and the cell type involved in the origin of these tumors are still unclear (46). The hypothesis stating that a subset of cells within the tumor, named cancer stem cells (CSCs), initiate and maintain tumor growth leading to a hierarchy of cells within GBM is now well accepted (9). The most recent form of the CSC model includes the concept of 'dynamic stemness', hypothesizing an interchange between CSCs and more-differentiated cells (progenitors) (24). In this sense, emerging findings support the existence of a contextually regulated equilibrium between CSCs and transit amplifying neoplastic progenitors, including the capacity of progenitor cells dedifferentiation to form CSCs (24).

These CSCs have functional similarities to normal neural stem cells (NSCs) including their clonogenicity and capability for multi-lineage differentiation (27, 46). Defined gradients of signaling factors coordinate self-renewal and differentiation in NSCs populations during neural development. Genetic alterations or epigenetic regulation of genes that disturb this delicate balance in NSCs and restricted progenitors may lead to development of brain tumors (53).

Bone morphogenetic proteins (BMPs) are a family of growth factors that mediate a wide variety of biological responses in NSC, ranging from proliferation and differentiation to apoptosis depending on the NSC developmental stage as well as the milieu of the local microenvironments (7, 25). It has been reported that BMP2/4 acts as a neuroepithelial proliferation signal at very early stages of embryonic central nervous system (CNS) development, an effect mediated principally by the Bone Morphogenetic Protein Receptor type IA (BMPRIA) (11, 35). Later in development, BMP2/4 induces neuronal and astrocytic differentiation of NSCs, an event that occurs via the Bone Morphogenetic Protein Receptor type IB (BMPRIB) (16, 29). In the adult brain stem cell niche, BMPs have an instructive role that favors the acquisition of an astroglial fate. Interestingly, a pro-differentiation BMP response mechanism seems to be preserved in some glioma CSCs. Furthermore, these cells express BMPRs, and BMP family ligands inhibit their proliferation. Importantly, transient *in vitro* exposure to BMP4 abolishes the capacity of transplanted GBM cells to establish intracerebral GBMs (38). However, BMPs RNA transcript production is regulated via promoter methylation/ hypermethylation and several reports have demonstrated that BMP gene methylation is associated with downregulated expression in different types of cancer (20, 52). Remarkably, epigenetic-mediated dysfunction of BMPR1B in a subset of GBM represses the pro-differentiation effects of BMPs (23).

While BMP signaling activation is crucial for many events in development, its inhibition is equally necessary for others. As a result, there are a number of extracellular and intracellular mechanisms that block the influence of BMP signaling. BMP actions are regulated *in vivo* by proteins such as Noggin, Follistatin,

Chordin, and Neurogenesin which antagonize BMPs activities by directly binding to BMPs ligands (6, 42). The endogenously secreted BMP antagonist, Noggin, limits BMP signaling below the gliogenic threshold and redirects normal stem cells to generate neurons (26). Therapy forcing glioma CSCs to differentiate might be a promising and notably non-cytotoxic strategy for CSC targeting. In this regard BMPs may be potential soluble factors in the treatment of gliomas (38).

In the present study, we established six glioma stem cell-enriched cell lines (GSC-ECLs) from tumor biopsies that exhibited cancer stem/progenitor cells properties and initiated tumor formation following xenotransplantation. We further demonstrated that not all GSC-ECLs responded equally to a particular differentiation stimuli. However, we found that BMP4 treatment decreased proliferation of all tested GSC-ECLs to a similar extent, even in the presence of mitogens.

As a whole, in the present study we determined that GSC-ECLs exhibit distinct preferences in lineage choice and possess a broad phenotypic plasticity which can be regulated by external factors. Moreover, the expressed phenotype may be largely determined by the interplay between the competence of the receiving cell (genetic and epigenetic signatures of individual GSC-ECL) and the signaling emerging from the surrounding microenvironment (niches). Therefore, further knowledge of the mechanisms that govern this interplay is needed to better control tumor growth.

Materials and Methods

Tissue samples

This study is in compliance with the October 2013 Helsinki Declaration and it has been approved by the Biomedical Research Ethics Committee "Comité de Ética en Investigaciones Biomédicas de la Fundación para la Lucha contra Enfermedades Neurológicas de la Infancia (FLENI)", and written informed consent was received from each patient whose tumor tissue was used for this project.

Fresh tumor specimens used for this study were surgically resected at FLENI. After resection, samples were snap-frozen and stored at -80°C. These sections were classified morphologically and graded according to WHO criteria by experienced neuropathologist (NA and GES).

Nucleic acid isolation

Fresh frozen human tissues from brain tumors or GSC-ECLs were used to extract high-molecular genomic DNA using DNeasy kit extraction (Qiagen, Valencia, CA, USA). Purified DNA was quantified by ultraviolet absorbance at 260 nm and DNA quality was assessed by electrophoresis on 1% agarose gels.

Genomic analysis

Genomic DNA was extracted from 1 to 5 mg frozen tissue or glioma-derived cells ($2x10^6$) as described above. Samples were quantified spectrophotometrically, and 5 ng of DNA were used in each determination. Loss of heterozigosity (LOH) was assessed by the QuMA method (32) using Applied Biosystems 7500 Real-Time PCR system. The following markers were studied: D1S468, D1S214 and D1S199 for 1p loss and D19S596, D19S408 and D19S867 for 19q loss. Markers for LOH at 10q were D10S536 (located near the phosphatase and tensin homolog, *PTEN*,

gene) and D10S1683 (mapping close to deleted in malignant brain tumors 1, *DMBT-1*, gene). Homozygous deletions in the cyclin-dependent kinase inhibitor 2A (*CDKN2A/ARF*) gene were detected following a published protocol (3). Epidermal growth factor receptor (*EGFR*) gene amplifications were assessed in a multiplex real-time reaction employing the same conditions described for *CDKN2A/ARF*, including Glyceraldehyde-3-phosphate dehydrogenase (*GAPDH*) as reference gene. Primers for the *EGFR* gene have the following sequences: forward 5′-GAAGCTTGCTGGTAGCACTTG-3′ and reverse 5′-GTGGAAGCCTTGAAGCAGAAC-3′; the probe has the following sequence: 5′-6FAMCCCAACTGTGAGCAAGGAGCACATAMRA-3′. *TP53* gene mutations (exons 5 to 8) were detected by direct sequencing using primers already described (47) and confirmed by direct sequencing. Isocitrate dehydrogenase 1 (*IDH1*), mutation screening was carried out according to the recently published method (30). O^6-methylguanine-DNA methyltransferase (MGMT) methylation-specific PCR Methylation status of *MGMT* gene was determined and validated by methylation-specific PCR (MSP) as previously described (34).

EGFRvIII detection

Total RNA was extracted from 50-100 mg of each frozen tumor specimen using TRIzol reagent (Invitrogen) in a tissue grinder and then treated with amplification grade DNase I for 15 minutes at 37°C. For each sample, 1 µg of total RNA was reverse transcribed using Superscript II (Invitrogen) with oligo(dT) priming according to the manufacturer's protocols. 2 µl of 1st strand cDNA ($1/10^{th}$ of the reverse transcription reaction volume) was then used as template in a 50 µl PCR

reaction containing 2 mM MgSO4, 0.2 µM of each primer, 0.2 mM dNTPs, 1x High Fidelity PCR Buffer, and 1 unit of Platinum Taq High Fidelity (Invitrogen).

Forward and reverse primer sequences to specifically amplify EGFR and EGFRvIII were 5' CTTCGGGGAGCAGCGATGCGA C 3' (spanning the 5' untranslated region and the beginning of exon 1) and 5' ACCAATACCTATTCCGTTACAC 3' (within exon 9), respectively. Cloned wild type EGFR and EGFRvIII cDNAs were used as templates in parallel positive control reactions, alongside reverse transcription and PCR negative control reactions. GAPDH was also amplified for each sample to assess relative RNA template quality and amount. Primers for GAPDH were 5' GTGAAGGTCGGAGTCAACGG 3' and 5' TGATGACAAGCTTCCCGTTCTC 3'.

Histological characterization

Biopsies from xenografts were processed for paraffin embedding and 10 µm thick sections were stained for Hematoxylin and Eosin. After deparaffinization, sections were microwaved in 10 mM sodium citrate buffer (pH 6.0) for 10 minutes and incubated with the primary antibody anti-GFAP (1:500, AB5804) (Millipore, Billerica, MA, USA), over night at 4C°. Antigen retrieval procedure was performed using citrate buffer and the microwave technique. Replacement of the primary antibody with phosphate buffer served as a negative control. Subsequently, slides were incubated with the appropriate secondary antibody and then with streptavidin/biotin peroxidase complex. Diaminobenzidine served as chromogen.

Ki-67 labeling of paraffin embedded sections was made with monoclonal antibody Ki67 (1:100, NCL-Ki67-MM1) (Novocastra Laboratories, Newcastle, UK). Briefly,

sections were deparaffinized, then placed in 300 ml of 10 mM citrate buffer (pH 6.0) and heated five times for 3 min each at full power in a 500-W microwave oven to activate the Ki-67 protein epitope. After heating, sections were reacted for 12 h with the primary antibody diluted 1:50 in phosphate-buffered saline containing 1% normal rabbit serum, stained by the avidin-biotin complex method, developed with methyl-green. More than 1000 cells were counted in several section areas that were as representative as possible of the pathological feature. Ki-67 labeling index was calculated as the percentage of positively stained nuclei.

Culture of human glioma-derived cells

Brain tumor cultures were established as soon as possible (20–30 min) after surgery by mechanical disaggregation of biopsies followed by accutase (Invitrogen, Carlsbad, CA, USA) incubation for 15 minutes at 37°C. Next, the cellular suspension was centrifuged for 5 minutes at 200x g. The resultant pellet was resuspended in serum-free medium consisting of Neurobasal medium supplemented with B27, N2, 20 ng/ml basic fibroblast growth factor (bFGF), 20 ng/ml epidermal growth factor (EGF), 2 mM L-glutamine, 2mM non-essential amino acids, 50 U/ml penicillin/streptomycin (all from Invitrogen, Carlsbad, CA, USA), 20µg/ml bovine pancreas insulin and 75 µg/ml low-endotoxin bovine serum albumin (Sigma, St. Louis, MO, USA) and plated onto laminin coated plates (10 ug/ml) (Sigma, St. Louis, MO, USA). Cells were routinely grown to confluence, dissociated using accutase and then splitted 1:2 to 1:3. Medium was replaced every 2–3 days.

To induce differentiation the same Neurobasal medium devoid of bFGF and EGF (growth factor withdrawal) was used. When indicated growth factor-deprived medium was supplemented with 0.5 ng/ml or 10 ng/ml human recombinant BMP4 and/or 250 ng/ml Noggin (R&D Systems, Minneapolis, MN, USA). Medium was replaced every 3–4 days.

Glioma stem cell-enriched cell lines transplantation

The tumorigenic potential of the cell lines was tested by orthotopic transplantation of 10^5 cells into the caudate-putamen of immunodeficient mice. All applicable international, national, and institutional guidelines for the care and use of animals were followed. Surgical procedures were carried out under general anesthesia with IP ketamine (0.1 mg/g body weight). We used 5-8 week old nude (*nu/nu*) mice. Mice were sacrificed within the first 4 months post-implantation. From each brain tumor sample several slices were cut, fixed and embedded in paraffin for pathological studies.

Immunostaining and fluorescent microscopy

Lineage and proliferation markers were analyzed by fluorescent microscopy. Briefly, cells were rinsed with ice-cold PBS containing Ca^{2+} and Mg^{2+} and fixed in PBSA (PBS with 0.1% bovine serum albumin) with 4% formaldehyde for 45 min. After two washes, cells were permeabilized with 0.1% Triton X-100 in PBSA with 10% normal goat serum for 30 min, washed twice and stained with the corresponding primary antibodies. Fluorescent secondary antibodies were used to locate the antigen/primary antibody complexes. Cells were counterstained with 4,

6-diamidino-2-phenylindole (DAPI) and examined under a Nikon Eclipse TE2000-S inverted microscope equipped with a 20X E-Plan objective and a super high-pressure mercury lamp. The images were acquired with a Nikon DXN1200F digital camera, which was controlled by the EclipseNet software (version 1.20.0 build 61). The following primary antibodies were used: anti-Sox2 (1:100, ab59776), anti-CD44 (1:100, ab19657) (Abcam Inc., Cambridge, UK); anti-Vimentin (1:200, M0725) (Dako, Glostrup, Denmark*)*; anti-Nestin (1:200, AB5922) (Chemicon International Inc., Temecula, CA, USA); anti-GFAP (1:500, AB5804) (Millipore*,* Billerica, MA, USA); anti-MAP2 (1:500, M1406); anti-α-Smooth muscle Actin (1:100, 1A4) (Sigma, St. Louis, MO, USA); anti-Ki67 (1:100, NCL-Ki67-MM1) (Novocastra Laboratories, Newcastle, UK).

Cell counting

Cells were counted in 6-8 random fields under inverted fluorescent microscope*:* Nikon Eclipse TE2000**-**S at 200x magnification, per experimental condition. The number of single- or double**-**stained cells was expressed as a percentage of the total DAPI-stained cell population.

Reverse Transcription Polymerase Chain Reaction

Total RNA was extracted using TRIzol reagent (Invitrogen, Carlsbad, CA, USA) according to manufacturer's instructions. cDNA was synthesized using MMLV reverse transcriptase (Promega, Madison, WI, USA) from 500 ng of total RNA. The cDNA samples were diluted fivefold and the PCR reaction was conducted at an annealing temperature of 60°C. Reactions were within the linear range of

amplification. Quantitative PCR studies were carried out using SYBR® Green-ER™ qPCR SuperMix UDG (Invitrogen, Carlsbad, CA, USA) and the primer sequences used are the following: CD133 sense 5'-ACAACACTACCAAGGACAAGG-3', antisense 5' GGACTTAATCTCATCAAGAACAGG-3'; GFAP sense 5'-AGGAAGATTGAGTCGCTGGAG-3', antisense 5'-CGGTGAGGTCTGGCTTGG-3'; MAP2 sense 5'-CAGGAGACAGAGATGAGAATTCCTT-3', antisense 5'-GTAGTGGGTGTTGAGGTACCACTCTT-3'; h-Caldesmon sense 5'-TGGAGGTGAATGCCCAGAAC-3', antisense 5'-GAAGGCGTTTTTGGCGTCTTT-3'; Calponin-1 sense 5'-CTGTCAGCCGAGGTTAAGAAC-3', antisense 5'-GAGGCCGTCCATGAAGTTGTT-3'; Transgelin sense 5'-AGTGCAGTCCAAAATCGAGAAG-3', antisense 5'-CTTGCTCAGAATCACGCCAT-3'; BMPR1A sense 5'-AGATGACCAGGGAGAAACCAC-3', antisense 5'-CAACATTCTATTGTCCGGCGTA-3'; BMPR1B sense 5'-GGAGCAGTGATGAGTGTCTAAGG-3', antisense 5'-TGCCCACAAACAGAAGAGTACC-3' and GAPDH sense 5'-ACAGCCTCAAGATCATCAG-3', antisense 5'-GAGTCCTTCCACGATACC-3'. All samples were analyzed using an ABI PRISM 7500 Sequence Detector System (PE Applied Biosystems, Foster City, CA, USA) and were normalized to gapdh gene expression.

Flow Cytometric Analysis

Single-cell suspensions were obtained by treatment with accutase (37°C for 5min). Cells ($1x10^6$) were incubated with monoclonal CD133/1 (AC133)-PE conjugate antibody (1:11, 130-080-801) (Miltenyi Biotec, Auburn, CA, USA) in PBS containing

0.5% bovine serum albumin and 2 mM EDTA for 10 min at 4°C and washed with 2 ml of PBS. Cells were then centrifuged at 300 x g for 5 min, resuspended in 0.5 ml PBS and analyzed by flow cytometry.

Data was acquired on a FACSAria II flow cytometer from Becton Dickinson (BD Biosciences, San Jose, USA) and analyzed using WinMDI 2.9 software. Background fluorescence was estimated by substituting the specific primary antibody with specific isotype controls.

Determination of cell doubling time

Proliferation rates were compared on the basis of doubling time. GSC-ECLs were plated in parallel at 100,000 or 200,000 cells per well in 6 well plates. After 7 and 14 days cells were enzymatically dissociated and counted using a hemacytometer. The increase in cell number compared to the initial number of cells was used to calculate the doubling time by assuming an exponential growth model. The two plating densities were chosen in order to minimize any effect of density dependent cell growth.

Western Blotting

Cells were lysed in ice-cold RIPA buffer supplemented with a protease inhibitor mixture, and protein concentration was determined using the Bicinchoninic Acid Protein Assay (Pierce™, Rockford, IL, USA). Equal amounts of protein were run on 12 % polyacrylamide gel electrophoresis, and transferred to PVDF-FL membrane (Millipore, Billerica, MA, USA). The membrane was blocked for 1 h in Odyssey

blocking buffer (LI-COR Biosciences, Lincoln, NE, USA) containing 0.1% Tween 20 and then incubated overnight at 4°C in a solution containing Odyssey blocking buffer, 0.05% Tween 20 and the corresponding primary antibodies. The membrane was washed 4 × 5 min with Tris-buffered saline (TBS), 20 mM Tris-HCl, pH 7.5, 500 mM NaCl) containing 0.1% Tween 20 (TTBS), then incubated for 1 h in a solution containing Odyssey blocking buffer, 0.2% Tween 20, and IR-Dye secondary antibodies (1:20.000, LI-COR Biosciences, Lincoln, NE, USA) and subsequently washed 4 × 5min in TTBS, 1 × 5min in TBS. The membrane was immediately scanned for protein bands using the 680nm and 780 nm channels at a scanning intensity of 4. Immunocomplexes were visualized using the Odyssey Infrared Imaging System (LI-COR). The following primary antibodies were used: anti-Actin (sc-1616; Santa Cruz, CA, USA), anti-BMPRIA (ABD51; Millipore, Billerica, MA, USA) Antigen/primary antibody complexes were detected with near infrared-fluorescence-labeled, IR-Dye 800CW or IR-Dye 680RD, secondary antibodies (LI-COR Biosciences, Lincoln, NE, USA).

Alternatively, after electrophoresis the separated proteins were transferred to a PVDF membrane (Bio-Rad, Hercules, CA, USA). Blots were blocked 1 h at room temperature in TTBS containing low-fat powdered milk (5%). Incubations with primary antibodies were performed at 4 °C for 12 h in blocking buffer (3% skim milk in TTBS). The membranes were then incubated with the corresponding counter-antibody and the proteins evidenced by enhanced chemiluminescence detection (SuperSignal West Femto System, Thermo Scientific, Rockford, IL, USA). The following primary antibodies were used: anti-Actin (sc-1616, Santa Cruz Biotechnology, Santa Cruz, CA, USA), anti-BMPR1B (SAB1403613; Sigma, St.

Louis, MO, USA). The following secondary antibodies were used: a horseradish peroxidase-conjugated α-rabbit IgG; α-mouse IgG or α-goat IgG.

BMP4 measurements

The concentration of BMP4 in the culture supernatants was determined using a specific Enzyme-Linked Immunosorbent Assay kit (# RAB0029, Sigma, St. Louis, MO, USA) following the manufacturer's instructions. Briefly, $4x10^5$ cells were seeded onto 24-well culture dishes and 300ul of medium per well were conditionated for 24 hs.

Results

GSC-ECLs conserve the genetic and epigenetic abnormalities present in their parental tumors, express neural/stem cell markers and initiate tumor formation following xenotransplantation

In this study, we isolated cells from high grade human glioma biopsies and cultured them as monolayers on laminin-coated plates in the presence of a glioma stem-permissive medium which contains EGF and bFGF (40). Currently, it is well accepted that under these conditions cultures are enriched in glioma stem cells (22). To test their long-term self-renewal capacity these cell lines were continuously passaged *in vitro* for more than one year. During this period GSC-ECLs retained their particular growth rate and morphology. The six established GSC-ECLs were named G02, G03, G05, G07, G08 and G09. All of them were derived from GBM samples. Basic demographic and clinical characteristics of each patient are described in table 1.

To elucidate whether the glioma derived cell lines were representative of their parent tumors at the molecular level, we evaluated several genetic and epigenetic alterations that are currently determined as part of the routine clinical interrogation of gliomas. To address this issue, we first evaluated codon 132 point mutations of the *IDH1* gene. Then, to further assess accumulation of genetic anomalies linked to tumor suppressor inactivation or mitogen hyperactivation, we analyzed *CDKN2A/ARF* gene homozygous deletion, LOH at 10q (associated to *PTEN* and *DMBT-1* inactivation), *TP53* gene mutations, *EGFR* gene amplification and presence of truncated *EGFR* variant mutation (*EGFRvIII*). Additionally, we determined the LOH for both 1p and 19q using at least three polymorphic markers on 1p and 19q each. Finally, promoter methylation status of the DNA repair gene that encodes the O^6-methylguanine-DNA methyltransferase (MGMT) was examined. As shown in table 2, our data confirmed that the derived cell lines highly conserved the genomic and epigenomic profiles of their parent tumors except for the observed *EGFR* amplifications. In accordance with previous reports, *EGFR* gene copies were decreased in almost all tested GSC-ECL with respect to the corresponding original tumor, suggesting that *in vitro* culture in the presence of recombinant EGF (20 ng/ml) selects against *EGFR* genetic lesions (44). Importantly, in this sense, no changes in G02 cell line were observed where chromosomal gain of the *EGFR* gene (trisomy 7) was detected.

Within the last few years, many efforts have been aimed to identify cell surface markers useful for prospective isolation of CSCs. Among these, much attention has been given to CD133/prominin-1, a cholesterol-binding membrane protein of unknown biological function. Currently, CD133 is used to enrich CSCs

from brain tumors (2, 38). Here, we evaluated CD133 transcript levels by quantitative RT-PCR analysis and found that they were highly variable among the tested GSC-ECLs (Fig. 1a, top panel). In all cases, flow cytometry analysis confirmed a strong correlation between CD133 mRNA levels and protein abundance and showed that in each cell line the fraction of positive cells ranged from 2.90±0.02% in G02 to 80.02±0.04% in G09 (Fig. 1a, mid and bottom panels). Importantly, it has been reported that certain high grade glioma-derived CD133 negative cells also display CSC properties, questioning the role of this trans-membrane protein as a unique marker of brain CSCs and highlighting the need for more specific markers (33).

Currently, to further draw the stemness signature of CSCs, the use of multiple markers such as the components of intermediate filaments, Nestin and Vimentin, the transmembrane glycoprotein, CD44, and the transcription factor sex determining region Y-box 2 (Sox2), is accepted. To ascertain whether glioma-derived cells have similarities to NSCs we undertook a phenotypic characterization of the isolated GSC-ECLs. By immunocytochemistry we determined the presence of the aforementioned NSC/neural progenitor markers. Nearly all cells within the cultures express Nestin, Vimentin, CD44 and Sox2 (Fig. 1b). Then, to test the capacity of GSC-ECLs to initiate tumor formation, 10^5 cells/mouse were injected into the right putamen of immunocompromised mice. After 2-4 months, mice were sacrificed revealing the formation of brain lesions exhibiting features of gliomas, which included human GFAP expression and a high proliferation index (Fig. 1c).

Finally, we estimated the doubling time of each GSC-ECL. Notably, a wide variation among cell lines was determined, which ranged from 2.97±0.18 days in G09 cells to 10.54±1.2 days in G05 cells (Fig. 1d).

GSC-ECLs exhibit distinct differentiation behaviors *in vitro*

Forcing differentiation of glioma stem cells may represent a potential effective therapeutic strategy; thus, it becomes increasingly important to understand how molecular signaling regulates differentiation of these cells. BMP4 is known to participate in the astrocytic differentiation of neural progenitor/stem cells (5). However, it has been reported that lineage choice of certain NSCs depends in part on BMPs concentrations (10). Therefore, to gain insight into GSC multipotent capacity, we exposed the six GSC-ECLs to three defined differentiating conditions that include: 1) growth factor (EGF and bFGF) withdrawal; 2) growth factor withdrawal plus BMP4 addition at low concentrations (0,5 ng/ml) and 3) growth factor withdrawal plus BMP4 addition at high concentrations (10 ng/ml).

Initially, to identify the phenotypes developed by these GSC-ECLs under the mentioned differentiating conditions, we stained cells with the astroglial marker, GFAP and with the neuronal marker, β-III-tubulin. Although in several reports this combination was used to follow-up both astroglial and neuronal differentiation (22, 23, 45), we found that GFAP was often co-expressed with β-III-tubulin, reflecting the abnormality of the glioma stem/progenitor cells phenotypes (14). Due to this aberrant expression, this double staining technique was ineffective to perform cell type identification (data not shown). After several approaches, we found that the combination of GFAP and MAP2 resulted more appropriate to discriminate cell

lineages. To this end, cells were counted according to their GFAP and MAP2 immunoreactivity and grouped as: $GFAP^-/MAP2^-$; $GFAP^+/MAP2^+$; $GFAP^+/MAP2^-$ and $GFAP^-/MAP2^+$. Despite a considerable percentage of $GFAP^+/MAP2^+$ cells were detected in some cases, this methodology allowed us to establish a tight correlation between lineage markers and morphology.

The six established GSC-ECLs exhibited different morphological aspects and underwent overt and distinct morphological changes after differentiation occurred. As detailed in table 3 and in figures 2 and 3, variations of recombinant BMP4 concentration (none; 0,5 ng/ml or 10 ng/ml) particularly influenced the differentiation outcome of each tested cell line. As expected, in some GSC-ECLs (G05 and G07) increasing concentrations of BMP4 favored the acquisition of an astroglial phenotype ($GFAP^+$ cells with a star-shaped and branched morphology) and prevented the appearance of neuronal-like cells ($MAP2^+$ cells with small cellular bodies and thin processes). In contrast, in G08 and G09 GSC-ECLs, cells only acquired an astrocyte-like fate upon growth factor removal or in the presence of low concentrations of BMP4 (0,5 ng/ml). It should be noted that in these cases, the addition of 0,5 ng/ml BMP4 further enhanced the astrocyte morphology and reduced the percentage of $MAP2^+$ cells. High concentrations of BMP4 (10 ng/ml), instead of promoting an astrocytic morphology, lead to the generation of homogeneous $GFAP^+$ cellular populations which displayed a flat and enlarged in size morphology. In these GSC-ECLs BMP4 also impaired neuronal differentiation in a concentration dependent manner. On the other hand, G03 cells under all differentiating conditions adopted an elongated cell shape with large and flat cytoplasm, similar to the one observed in G08 and G09 cell lines under high

concentrations of BMP4. After differentiation onset, this cell line also displayed an increase in the number of $GFAP^+$ cells, which became more evident in the presence of high concentrations of BMP4. Additionally, under all culture conditions, $MAP2^+$ cells were barely detectable. Finally, G02-differentated cells acquired a heterogeneous appearance which was accompanied by an increase in both lineage markers. However, in none of these differentiating conditions G02 cells adopted a predominant phenotype.

Remarkably, before subjecting GSC-ECL to differentiating stimuli, we found that in several cell lines (G02; G03; G07 and G09) GFAP and MAP2 levels were low or undetectable, even though in some of them (G05 and G08) these markers were highly expressed. Nonetheless, in these cell lines (G05 and G08) the differentiation process was evidenced by dramatic morphological changes. In consequence, it should be noted that an increase of lineage marker expression not always can be considered as a feature of glioma stem-cell differentiation (Fig. 2 and Fig. 3).

The differentiation effects of each experimental condition were also evaluated by quantitative RT-PCR analysis. As shown in figure 4a (top panel) the expression levels of GFAP mRNA of all GSC-ECLs were significantly induced in the tested differentiating conditions, being more pronounced in the presence of 10 ng/ml recombinant BMP4. This induction correlates with the determined increase in the percentage of $GFAP^+$ cells under the corresponding conditions (Fig. 2 and 3, right panels). With respect to MAP2 expression levels, we found that in G02, G05 and G09 cell lines growth factor withdrawal led to an induction of this transcript. Conversely, the presence of BMP4 at high concentrations caused a significant

decrease in the levels of this mRNA in G03, G07, G08 and G09 cell lines (Fig. 4a, bottom panel). This changes are in accordance with the reduction of the percentage of $MAP2^+$ cells observed when cells were exposed to recombinant BMP4 at 10 ng/ml (Fig. 2 and 3, right panels).

Finally, by flow cytometry we determined that in G08 and G09 the percentage of $CD133^+$ cells diminished at 21 days of differentiation onset (both under growth factor withdrawal and under growth factor withdrawal plus BMP4 addition at 10 ng/ml), although no significant changes were observed in G07 (Fig. 4b).

Taken together, these results further demonstrate the well known inter-tumoral heterogeneity exhibited in high grade gliomas, which was manifested both at their undifferentiated state as well as at their differentiation capacity.

Noggin decreases the ratio of $GFAP^+$ to $MAP2^+$ cells in GSC-ECLs

In line with previous reports (10, 39), we found that in all differentiated GSC-ECLs, BMP4 addition caused a dose-dependent increase in the number of $GFAP^+$ cells and a reduction in the percentage of $MAP2^+$ cells (Fig. 2 and 3, bottom panels), supporting the concept that this morphogen is acting as an astroglial inducer. However, in the absence of both recombinant BMP4 and growth factors, we also detected the appearance of large populations of $GFAP^+$ astrocyte-like cells (mainly in G08 and G09 cell lines). Therefore, it stands to reason that this adopted phenotype could be due to an autocrine/paracrine BMP signaling. If so, the presence of recombinant Noggin would reduce the availability of endogenous

BMPs below the gliogenic threshold and allow neuronal differentiation to proceed (astroglial-neuronal switch).

To explore this possibility, we first studied the cellular response triggered in G08 and G09 cell lines after Noggin exposure in the absence of mitogens during 21 days. Interestingly, the presence of Noggin produced a decrease in GFAP expression levels, a marked reduction in the percentages of $GFAP^+$ cells, and more important, it impaired the appearance of process-bearing star-shaped cells. Concomitantly, an increase in the fraction of $MAP2^+$ neuronal-like cells was also observed (Fig. 5). Thus, these results suggest that the presence of recombinant Noggin could be impairing astroglial differentiation by reducing the action of endogenous BMP ligands (e.g. BMP2, BMP4, etc) which might be secreted by these GSC-ECLs. In this sense, the mere depletion of growth factors could lead to the release of an endogenous BMPs signaling, that in turn will possibly allow astrocytic fate commitment. However, it should be noted that growth factor withdrawal led to specific lineage choices in each of these six GSC-ECLs (Fig. 2 and 3), suggesting that the molecular profile of individual GSC-ECL would ultimately set the threshold that determines the final phenotype in response to differentiating signals coming from tumor microenvironment (niche).

To gain insight into this phenomenon, and especially considering that G03 cell line was not able to give rise to $MAP2^+$ cells in any of the assayed experimental conditions, we exposed this cell line to recombinant Noggin. Notably, in the absence of growth factors, the addition of this BMP antagonist led to the appearance of a considerable fraction of $MAP2^+$ cells. However, the majority of these $MAP2^+$ cells did not acquire a neuron-like morphology, suggesting that in this

cell line, neuronal differentiation is somehow impaired, at least in the assayed conditions (Fig. 5, bottom panel).

Finally, to explore if the observed plasticity can occur in the presence of mitogens, we cultured these proliferating GSC-ECLs for 21 days in growth factor-containing media, supplemented with Noggin (250 ng/ml) or with BMP4 (10 ng/ml). As shown in figure 6, in these conditions the presence of Noggin did not produce significant changes in cell morphology, although it led to an increase in the fraction of $MAP2^+$ cells, which was accompanied by a decrease in $GFAP^+$ population. On the contrary, the addition of recombinant BMP4 to growth factor-containing media increased the percentage of $GFAP^+$ cells and practically abolished the presence of $MAP2^+$ cells. Therefore, even under conditions that allow proliferation (presence of bFGF and EGF); the phenotype of these GSC-ECLs can be modulated by the status of the BMP signaling network.

Particular GSC-ECLs are capable of adopting a smooth muscle-like phenotype

Neural stem cells display a broad differentiation potential that is not restricted to tissues of ectodermal origin but includes muscle and endothelial lineages. Such plasticity is lost during the transition from stem to progenitor cells and not regained during terminal differentiation (4, 8, 15). Moreover, isolated CNS stem cells exposed to novel environments can differentiate into both CNS as well as non-CNS fates (4, 15). Thus, differentiation appears to be dependent on the environment around stem cells and diffusible signals seem to be important in the regulation of fate choice. An example of this is the promotion of cortical stem cell

differentiation into alpha smooth muscle actin (α-SMA)-positive cells exerted by BMP4 (>10 ng/ml) (10).

The above considerations, together with the morphological changes (spread cells with enlarged cytoplasm) observed in G03 cell lines under all the differentiation conditions and in G08 and G09 cell lines in the presence of high concentrations of BMP4, prompted us to determine if GSC-ECLs have the potential to differentiate into a smooth muscle-like phenotype. To explore this possibility, we labeled cells with the cytoskeletal protein, α-SMA.

The six GSC-ECLs exhibited very dissimilar results with respect to α-SMA immunoreactivity. In all tested conditions G02, G05 and G07 cell lines were negative for this marker, while G03, G08 and G09 cell lines exhibited different percentages of α-SMA$^+$ cells. As shown in figure 7, the morphological changes displayed by G03 cell line under all tested differentiation conditions were accompanied by the formation of α-SMA fibers. However high doses of BMP4 was the only differentiating condition studied that gave rise to significant percentages of α-SMA$^+$ cells in G08 and G09 cell lines (Fig. 7a). Finally, by double-labeling experiments we determined that a considerable subset of G03 and G09 cells co-expressed α-SMA and GFAP (Fig. 7b).

To further characterize the adopted smooth muscle-like phenotype we determined the mRNA expression levels of three smooth muscle markers: h-Caldesmon, Calponin-1 and Transgelin/Smooth muscle protein 22-alpha in G03, G05 and G09 cell lines (1, 19, 43). Quantitative RT-PCR analysis revealed a strong induction of these three genes in G03 cells under all differentiating conditions as well as in G09 cells when differentiated in the presence of high concentration of

recombinant BMP4. Notably, the mRNA expression levels of these genes in each cell line tightly correlated with their capacity to adopt a smooth muscle-like phenotype (Fig. 7c). In fact, G05 cell line, which never adopted a smooth muscle-like phenotype under the tested differentiating conditions, displayed very low levels of these transcripts (Fig. 7c).

Interestingly, in our initial attempts to identify the cellular phenotypes adopted by GSC-ECLs under differentiation conditions, we found that G03 cell line maintained a strikingly high percentage of $GFAP^-/MAP2^-$ cells (Fig 2, bottom panel). This behavior was also observed in G09 line under high concentrations of recombinant BMP4, in which the percentage of $GFAP^-/MAP2^-$ cells further increased with respect to the other experimental conditions (Fig. 3, bottom panel). One explanation for these results could be that under the aforementioned conditions these cell lines failed to differentiate. However, as in each cell line the percentages of $GFAP^-/\alpha\text{-}SMA^+$ cells were very similar to those determined previously for $GFAP^-/MAP2^-$ cells, it is reasonable to speculate that a great proportion of these double negative populations may actually correspond to the herein characterized $GFAP^-/\alpha\text{-}SMA^+$ fraction (Fig. 7b).

GSC-ECLs reduce their proliferative activity upon exposure to differentiating conditions

The phenotypic diversity displayed by GSC-ECLs subjected to the abovementioned differentiation protocols prompted us to explore whether these differences would be reflected in their proliferative responses. To address this

issue, we measured the Ki67 positive cell fraction in GSC-ECLs exposed to distinct experimental conditions by immunostaining.

As shown in figure 8, in the presence of bFGF and EGF, which favors the self-renewal and proliferation of the stem cell compartment, the percentage of $Ki67^+$ cells was highly variable, ranging from approximately 30% in G05 cell line to 67% in G09 cell line. Accordingly, this variability tightly correlates with the doubling time of each cell line (Fig. 1d). Importantly, under all tested differentiating conditions, a significant reduction in the proliferative ability was determined. However, a more pronounced decrease in cell division was achieved after cells were treated with 10 ng/ml BMP4, even in the presence of bFGF and EGF. These findings suggest that BMP4 itself could counteract growth factor proliferative stimuli.

G09 cell line was the only one whose proliferative activity was tightly dependent on bFGF and EGF presence, as we found that Ki67 immunorreactivity in growth factor deprived-cells was comparable to the observed in the presence of 10 ng/ml BMP4. It should be noted that this cell line exhibited neither EGFR gene amplification nor EGFRvIII mutation, contrary to what was determined in the rest of the GSC-ECLs (Table 2).

In contrast to the elevated variability observed in GSC-ECLs differentiation patterns, we found that recombinant BMP4 treatment (even in the presence of bFGF and EGF) led to a similar decrease of cellular proliferation in all tested cell lines. This suggests that BMP4 action is accomplished through signals that differentially modulate proliferation and differentiation processes.

BMP signaling status influences the lineage choice of GSC-ECLs

To gain insight into the molecular determinants that ultimately dictate the lineage choice, we first characterized the expression profile of BMPRs in the six isolated GSC-ECLs. By quantitative RT-PCR and Western blot analysis we determined that each cell line exhibits a specific expression pattern. We find that all undifferentiated cell lines show comparable expression levels of BMPR1A but very different expression levels of BMPR1B (Fig. 9a and b and data not shown). These differences in BMPR1B abundance prompted us to explore whether the expression levels of this receptor change upon differentiation or in response to differentiating stimulus. By quantitative RT-PCR analysis we find that, growth factor withdrawal and BMP4 addition at a low concentration (0.5 ng/ml) led to the induction of BMPR1B transcript levels in all studied cell lines. However, when recombinant BMP4 was added at a high concentration (10 ng/ml) different behaviors were observed. While in G02, G03 and G05 cell lines BMPR1B mRNA expression levels increased, in G07 cell line no appreciable changes were observed. Contrarily, in G08 and G09 cell lines mRNA levels were significantly reduced (Fig. 9c). Similar results were obtained by Western blotting (Fig. 9d).

Interestingly, cell lines that expressed higher levels of BMPR1B were the ones (G05, G08 and G09) that preferentially adopted an astrocyte-like phenotype when differentiated in the absence of growth factors or in the absence of growth factors plus BMP4 at a low concentration (0.5 ng/ml) (Fig. 2 and 3). Remarkably, under differentiating conditions, where BMPR1B expression levels were induced, these cell lines acquired an astrocyte-like phenotype. In contrast, when BMPR1B transcript levels were reduced, as observed in G08 and G09 cell lines in the

presence of 10 ng/ml BMP4, a smooth muscle-like phenotype was adopted (Fig. 7a).

G03 and G07 cell lines express similar low levels of BMPR1B, even though they committed to different lineages (smooth muscle-like and neuronal-like phenotypes respectively). Thus, their respective BMPR1B expression levels do not account for the different phenotypes adopted by these cell lines. In an attempt to understand these differences, we measured the abundance of endogenous BMP4 in undifferentiated GSL-ECLs culture supernatants. Notably, we find that in G03 cell line, secreted BMP4 was significantly more abundant than in the rest of the studied cell lines. This pattern was also observed in growth factor deprived cell lines (Fig. 9e). Moreover, a significant increase in the abundance of secreted BMP4 was detected in G03, G08 and G09 GSC-ECLs when they were differentiated in the absence of growth factors for 21 days (Fig. 9e). The higher concentration of endogenous BMP4 determined in G03 cells supernatants suggests that the abundance of this morphogen could be responsible, at least in part, for the smooth muscle-like phenotype adoption. It is important to note that the same molecular setting (high levels of BMP4 and low expression of BMPR1B) was present when G08 and G09 cell lines exhibited a smooth muscle-like phenotype (Fig. 7a).

Analyzing this together, we noted a correlation between BMP4 and BMPR1B expression levels and the lineage adopted when growth factors were removed. While astrocyte-like phenotypes are preferentially adopted by cells that express high levels of BMPR1B (G05, G08 and G09 cell lines), smooth muscle-like phenotypes are acquired in cells that show low levels of BMPR1B and are exposed

to high concentrations of BMP4 (G03 cell line). Finally, a neuronal-like phenotype is adopted by G07 GSC-ECL, which expresses low levels of BMPR1B but secretes lower amounts of BMP4 than G03 cell line.

Discussion

Since it has been clearly demonstrated that distinct adult NSCs and progenitors exist (49), it is conceivable to think that a particular GSC phenotype may account for the cellular origin of the tumor. However, it has been proposed that lineage marker expression is not necessarily indicative of the cancer cell of origin (21, 56). For instance, it was observed that breast cancer cells displaying a phenotype of basal cells would originate from luminal cells (31). Moreover, in some cancer cells a certain degree of “phenotypic reversibility” has been determined, wherein particular cell types may acquire CSC properties. This phenomenon could be induced by microenvironment-secreted growth factors and/or by stress signals (51). In gliomas, the induction of the hypoxia-inducible factor 2 alpha (HIF2α) transcription factor, which mediates the transcriptional response to hypoxia, has been involved in the acquisition of GSC properties and in the up-regulation of CD133 expression (17).

In this work we observed that different GSC-ECLs show particular phenotypes. However, we have determined that these cells (under proliferating conditions) can change their lineage marker expression pattern and their morphology in response to the BMP/Noggin signaling status. Although it is possible that tumor cells retain certain phenotypic traits present in the cancer cell of origin, these results suggest that the interaction between the molecular setting of each

GSC-ECL and the micro-environmental signals plays a key role in the phenotypic outcome of a given CSC. Therefore, it should be noted that under particular experimental conditions, an *in vitro* GSC phenotype might be biased.

As it has been established, BMPs act as potent anti-mitogenic agents in GSCs (38). In the present study we further confirm this phenomenon, as all studied GSC-ECLs exposed to this morphogen significantly reduced their proliferative capacity, even in the presence of mitogens (Fig. 8). Therefore, it is possible to infer that the presence of BMP antagonists within the tumor microenvironment could favor CSC proliferation. In this sense, Yan and coworkers recently reported that the BMP inhibitor, Gremlin1, is secreted in a CSC-specific manner to promote their maintenance within the tumor hierarchy (55).

Although the effect of growth factor withdrawal and/or recombinant BMP4 addition over cellular proliferation was similar in all tested GSC-ECLs, each of these cell lines showed a specific differentiation pattern. While under certain conditions some GSC-ECLs gave rise to cultures with high proportions of neuronal-like cells (G07 and G09), others showed a high tendency to generate astrocyte-like cells (G05 and G08). Contrarily, G03 always resulted in homogeneous cell populations showing a smooth muscle-like phenotype. Moreover, these cell lines displayed cell line specific ranges of phenotypic plasticity, as the adopted phenotype was largely dependent on the differentiation conditions, possibly reflecting a varying degree of multipotency among different GSC-ECLs. Herein, we find that the expression levels of both BMP4 and BMPR1B would be critical determinants of the ultimate lineage choice. Importantly, the mere deprivation of growth factors led to an increase in the levels of BMPR1B which in some GSC-

ECLs (G03, G08 and G09) was accompanied by a rise in the abundance of secreted BMP4. These results suggest that the absence of exogenous bFGF and EGF could allow the activation of the BMP axis involved in glioma differentiation. In this regard, it has been reported that during neural development, FGF signaling downregulates BMP4 and BMP7 expression (18, 54) and negatively regulate Smad phosphorylation to inhibit downstream BMP signaling(36, 37).

In parallel with growth of the brain, rapid angiogenesis is necessary to supply nutrients and oxygen. Recent studies have shown that neural progenitor cells isolated from rat embryonic cerebral cortex can differentiate into smooth muscle cells when stimulated with fetal bovine serum, suggesting a contribution to the generation of blood vessels in the brain. (50). Additionally, it has been reported that lineage choice in cortical NSCs strongly depends on extracellular signals such as BMP4, Ciliary neurotrophic factor (CNTF) and Brain-derived neurotrophic factor (BDNF) (10). In this publication the authors found that, although low concentrations of BMP4 promote both neuronal and astroglial differentiation, higher doses of this morphogen lead to development of smooth muscle-like cells. In this regard, we also found that BMP4 induces differentiation of GSC-ECLs in a dose-dependent manner. For instance, some GSC-ECLs that differentiated into astrocytes or neurons in the presence of low doses of BMP4, adopted a smooth muscle-like phenotype when exposed to higher doses of this ligand (10 ng/ml). Therefore, despite their tumoral nature, these GSC-ECLs seem to preserve certain differentiation pathways present in particular NSCs. It is conceivable that under specific environmental stimuli, glioma CSCs may activate a latent program of smooth muscle differentiation to promote neovascularization and support tumor

growth. In fact, Rajan and coworkers described that BMP4 causes the activation of at least two distinct cytoplasmic signaling pathways in neural stem cells, one mediated by SMAD proteins and the other by signal transducer and activator of transcription (STAT) proteins (41). They found that in cultures with low basal levels of activated STAT proteins, BMP4 induces smooth muscle differentiation by activating Smad1/5/8. Conversely, in cultures that show higher basal levels of activated STAT proteins, BMP4 further activates STAT proteins to generate glia at the expense of smooth muscle. It will be of interest to see if these signaling pathways are operative in glioma CSCs too. If so, the basal levels of activated STAT proteins present in each GSC-ECL would be another determinant of cell fate choice upon differentiation stimuli.

Recent evidence suggests that the stem cell fraction of gliomas is radio-resistant, shows preferential activation of DNA damage checkpoint responses, has an increased DNA repair capacity and is enriched following radiation (2). Consequently, therapies acting through the induction of apoptosis, which largely includes radio and chemotherapies, may have lethal effects on the majority of the amplifying cell population but lesser effects on the stem cell-based regenerative capacity of tumors. Although differentiation therapy does not directly destroy neoplastic stem cells, it restrains their growth and prevents them from generating more proliferating or transit amplifying progenitor cancer cells. Thus, forcing tumor cells to differentiate constitutes an emerging concept in the search for alternative cancer therapies. In this sense, it has been reported that BMP ligands can abolish brain cancer stem cell (BCSC) population by inducing stem cells to undergo differentiation (38). Notwithstanding, Lee and colleagues (23) found that BMPs

facilitate proliferation rather than differentiation in a subset of BCSCs by epigenetic silencing of the BMPRIB gene. These distinct responses once more highlight the importance of characterizing the molecular features of individual CSCs populations. Importantly, in this study we have established that, regardless of their molecular signatures, all tested GSC-ECLs markedly reduced their proliferation rates when they were exposed to differentiating conditions, mostly in presence of high BMP4 concentrations.

Results presented herein beg the question of how extrinsic signals can control CSC fate in such diverse and unexpected ways and highlight the importance of this *in vitro* model. Likewise, the suggestion that BMP4 might be explored as a potential therapeutic agent should be viewed with caution given the previous demonstration of its mitogenic effects in a subset of BCSCs (23) and our findings that, under determined conditions and molecular settings, this morphogen may lead to the adoption of phenotypes that might favor tumor sustaining capacity (12). The ability to correctly predict the outcome triggered by a differentiating agent would influence treatment decisions. Thus, a thorough molecular characterization of these patient-derived GSC-ECLs offer the possibility to predict *a priori*, for instance, the effect on the proliferative activity or on the acquisition of a phenotype under a particular differentiating therapy, providing a rationale to develop and test antineoplastic drugs. Furthermore, the fact that the adoption of a determined phenotype can be modulated by endogenous antagonists of the differentiating agent further expands this rationale.

Acknowledgments

This work was supported by research grants from Agencia Nacional de Promoción Científica y Tecnológica (ANPCYT) (PID2007-00112 and PID2007-00111), Instituto Nacional del Cáncer (INC) (INC UN 0170046) and Fundación para la Lucha contra las Enfermedades Neurológicas de la Infancia (FLENI). We gracefully acknowledge Dr. Andrés Cervio (Neurosurgery Department, FLENI) for his cooperation and Dra. Blanca Diez (Neurooncology Department, FLENI) for many helpful discussions. We also would like to thank Carolina Bluguermann for her collaboration in murine injections, to Olivia Morris, to Claus von Hessert-Vaudoncourt and Miguel Riudavetz for their cooperation with manuscript preparation and to Marcelo Schultz and Estefania Rojas for their skillful technical assistance.

Conflict of interest

The authors declare that they have no conflict of interest.

References

1. Assinder SJ, Stanton JA, Prasad PD (2009) Transgelin: an actin-binding protein and tumour suppressor. Int J Biochem Cell Biol.41(3):482-6.
2. Bao S, Wu Q, McLendon RE, Hao Y, Shi Q, Hjelmeland AB, Dewhirst MW, Bigner DD, Rich JN (2006) Glioma stem cells promote radioresistance by preferential activation of the DNA damage response. Nature.444(7120):756-60.
3. Berggren P, Kumar R, Sakano S, Hemminki L, Wada T, Steineck G, Adolfsson J, Larsson P, Norming U, Wijkstrom H, Hemminki K (2003) Detecting homozygous deletions in the CDKN2A(p16(INK4a))/ARF(p14(ARF)) gene in urinary bladder cancer using real-time quantitative PCR. Clin Cancer Res.9(1):235-42.
4. Bjornson CR, Rietze RL, Reynolds BA, Magli MC, Vescovi AL (1999) Turning brain into blood: a hematopoietic fate adopted by adult neural stem cells in vivo. Science.283(5401):534-7.
5. Bonaguidi MA, McGuire T, Hu M, Kan L, Samanta J, Kessler JA (2005) LIF and BMP signaling generate separate and discrete types of GFAP-expressing cells. Development.132(24):5503-14.
6. Bonaguidi MA, Peng CY, McGuire T, Falciglia G, Gobeske KT, Czeisler C, Kessler JA (2008) Noggin expands neural stem cells in the adult hippocampus. J Neurosci.28(37):9194-204.

7. Bond AM, Bhalala OG, Kessler JA (2012) The dynamic role of bone morphogenetic proteins in neural stem cell fate and maturation. Dev Neurobiol.72(7):1068-84.
8. Clarke DL, Johansson CB, Wilbertz J, Veress B, Nilsson E, Karlstrom H, Lendahl U, Frisen J (2000) Generalized potential of adult neural stem cells. Science.288(5471):1660-3.
9. Clevers H (2011) The cancer stem cell: premises, promises and challenges. Nat Med.17(3):313-9.
10. Chang MY, Son H, Lee YS, Lee SH (2003) Neurons and astrocytes secrete factors that cause stem cells to differentiate into neurons and astrocytes, respectively. Mol Cell Neurosci.23(3):414-26.
11. Chen HL, Panchision DM (2007) Concise review: bone morphogenetic protein pleiotropism in neural stem cells and their derivatives--alternative pathways, convergent signals. Stem Cells.25(1):63-8.
12. Cheng L, Huang Z, Zhou W, Wu Q, Donnola S, Liu JK, Fang X, Sloan AE, Mao Y, Lathia JD, Min W, McLendon RE, Rich JN, Bao S (2013) Glioblastoma stem cells generate vascular pericytes to support vessel function and tumor growth. Cell.153(1):139-52.
13. DeAngelis LM (2001) Brain tumors. N Engl J Med.344(2):114-23.
14. Galli R, Binda E, Orfanelli U, Cipelletti B, Gritti A, De Vitis S, Fiocco R, Foroni C, Dimeco F, Vescovi A (2004) Isolation and characterization of tumorigenic, stem-like neural precursors from human glioblastoma. Cancer Res.64(19):7011-21.
15. Galli R, Borello U, Gritti A, Minasi MG, Bjornson C, Coletta M, Mora M, De Angelis MG, Fiocco R, Cossu G, Vescovi AL (2000) Skeletal myogenic potential of human and mouse neural stem cells. Nat Neurosci.3(10):986-91.
16. Hall AK, Miller RH (2004) Emerging roles for bone morphogenetic proteins in central nervous system glial biology. J Neurosci Res.76(1):1-8.
17. Heddleston JM, Li Z, McLendon RE, Hjelmeland AB, Rich JN (2009) The hypoxic microenvironment maintains glioblastoma stem cells and promotes reprogramming towards a cancer stem cell phenotype. Cell Cycle.8(20):3274-84.
18. Ishimura A, Maeda R, Takeda M, Kikkawa M, Daar IO, Maeno M (2000) Involvement of BMP-4/msx-1 and FGF pathways in neural induction in the Xenopus embryo. Development, growth & differentiation.42(4):307-16.
19. Kim HR, Appel S, Vetterkind S, Gangopadhyay SS, Morgan KG (2008) Smooth muscle signalling pathways in health and disease. J Cell Mol Med.12(6A):2165-80.
20. Kimura K, Toyooka S, Tsukuda K, Yamamoto H, Suehisa H, Soh J, Otani H, Kubo T, Aoe K, Fujimoto N, Kishimoto T, Sano Y, Pass HI, Date H (2008) The aberrant promoter methylation of BMP3b and BMP6 in malignant pleural mesotheliomas. Oncol Rep.20(5):1265-8.
21. Lapouge G, Youssef KK, Vokaer B, Achouri Y, Michaux C, Sotiropoulou PA, Blanpain C (2011) Identifying the cellular origin of squamous skin tumors. Proc Natl Acad Sci U S A.108(18):7431-6.
22. Lee J, Kotliarova S, Kotliarov Y, Li A, Su Q, Donin NM, Pastorino S, Purow BW, Christopher N, Zhang W, Park JK, Fine HA (2006) Tumor stem cells derived from glioblastomas cultured in bFGF and EGF more closely mirror the phenotype and genotype of primary tumors than do serum-cultured cell lines. Cancer Cell.9(5):391-403.
23. Lee J, Son MJ, Woolard K, Donin NM, Li A, Cheng CH, Kotliarova S, Kotliarov Y, Walling J, Ahn S, Kim M, Totonchy M, Cusack T, Ene C, Ma H, Su Q, Zenklusen JC, Zhang W, Maric D, Fine HA (2008) Epigenetic-mediated dysfunction of the bone morphogenetic protein pathway inhibits differentiation of glioblastoma-initiating cells. Cancer Cell.13(1):69-80.
24. Li Y, Laterra J (2012) Cancer stem cells: distinct entities or dynamically regulated phenotypes? Cancer Res.72(3):576-80.

25. Lim DA, Tramontin AD, Trevejo JM, Herrera DG, Garcia-Verdugo JM, Alvarez-Buylla A (2000) Noggin antagonizes BMP signaling to create a niche for adult neurogenesis. Neuron.28(3):713-26.
26. Liu C, Tian G, Tu Y, Fu J, Lan C, Wu N (2009) Expression pattern and clinical prognostic relevance of bone morphogenetic protein-2 in human gliomas. Jpn J Clin Oncol.39(10):625-31.
27. Lobo NA, Shimono Y, Qian D, Clarke MF (2007) The biology of cancer stem cells. Annu Rev Cell Dev Biol.23:675-99.
28. Maher EA, Furnari FB, Bachoo RM, Rowitch DH, Louis DN, Cavenee WK, DePinho RA (2001) Malignant glioma: genetics and biology of a grave matter. Genes Dev.15(11):1311-33.
29. Mehler MF, Mabie PC, Zhu G, Gokhan S, Kessler JA (2000) Developmental changes in progenitor cell responsiveness to bone morphogenetic proteins differentially modulate progressive CNS lineage fate. Dev Neurosci.22(1-2):74-85.
30. Meyer J, Pusch S, Balss J, Capper D, Mueller W, Christians A, Hartmann C, von Deimling A (2010) PCR- and restriction endonuclease-based detection of IDH1 mutations. Brain Pathol.20(2):298-300.
31. Molyneux G, Geyer FC, Magnay FA, McCarthy A, Kendrick H, Natrajan R, Mackay A, Grigoriadis A, Tutt A, Ashworth A, Reis-Filho JS, Smalley MJ (2010) BRCA1 basal-like breast cancers originate from luminal epithelial progenitors and not from basal stem cells. Cell Stem Cell.7(3):403-17.
32. Nigro JM, Takahashi MA, Ginzinger DG, Law M, Passe S, Jenkins RB, Aldape K (2001) Detection of 1p and 19q loss in oligodendroglioma by quantitative microsatellite analysis, a real-time quantitative polymerase chain reaction assay. Am J Pathol.158(4):1253-62.
33. Ogden AT, Waziri AE, Lochhead RA, Fusco D, Lopez K, Ellis JA, Kang J, Assanah M, McKhann GM, Sisti MB, McCormick PC, Canoll P, Bruce JN (2008) Identification of A2B5+CD133- tumor-initiating cells in adult human gliomas. Neurosurgery.62(2):505-14; discussion 14-5.
34. Palmisano WA, Divine KK, Saccomanno G, Gilliland FD, Baylin SB, Herman JG, Belinsky SA (2000) Predicting lung cancer by detecting aberrant promoter methylation in sputum. Cancer Res.60(21):5954-8.
35. Panchision DM, Pickel JM, Studer L, Lee SH, Turner PA, Hazel TG, McKay RD (2001) Sequential actions of BMP receptors control neural precursor cell production and fate. Genes Dev.15(16):2094-110.
36. Pera EM, Ikeda A, Eivers E, De Robertis EM (2003) Integration of IGF, FGF, and anti-BMP signals via Smad1 phosphorylation in neural induction. Genes Dev.17(24):3023-8.
37. Pera EM, Wessely O, Li SY, De Robertis EM (2001) Neural and head induction by insulin-like growth factor signals. Developmental cell.1(5):655-65.
38. Piccirillo SG, Reynolds BA, Zanetti N, Lamorte G, Binda E, Broggi G, Brem H, Olivi A, Dimeco F, Vescovi AL (2006) Bone morphogenetic proteins inhibit the tumorigenic potential of human brain tumour-initiating cells. Nature.444(7120):761-5.
39. Piccirillo SG, Vescovi AL (2006) Bone morphogenetic proteins regulate tumorigenicity in human glioblastoma stem cells. Ernst Schering Found Symp Proc. (5):59-81.
40. Pollard SM, Yoshikawa K, Clarke ID, Danovi D, Stricker S, Russell R, Bayani J, Head R, Lee M, Bernstein M, Squire JA, Smith A, Dirks P (2009) Glioma stem cell lines expanded in adherent culture have tumor-specific phenotypes and are suitable for chemical and genetic screens. Cell Stem Cell.4(6):568-80.
41. Rajan P, Panchision DM, Newell LF, McKay RD (2003) BMPs signal alternately through a SMAD or FRAP-STAT pathway to regulate fate choice in CNS stem cells. J Cell Biol.161(5):911-21.
42. Rider CC, Mulloy B (2010) Bone morphogenetic protein and growth differentiation factor cytokine families and their protein antagonists. Biochem J.429(1):1-12.

43. Rozenblum GT, Gimona M (2008) Calponins: adaptable modular regulators of the actin cytoskeleton. Int J Biochem Cell Biol.40(10):1990-5.
44. Schulte A, Gunther HS, Martens T, Zapf S, Riethdorf S, Wulfing C, Stoupiec M, Westphal M, Lamszus K (2012) Glioblastoma stem-like cell lines with either maintenance or loss of high-level EGFR amplification, generated via modulation of ligand concentration. Clin Cancer Res.18(7):1901-13.
45. Singh SK, Clarke ID, Terasaki M, Bonn VE, Hawkins C, Squire J, Dirks PB (2003) Identification of a cancer stem cell in human brain tumors. Cancer Res.63(18):5821-8.
46. Singh SK, Hawkins C, Clarke ID, Squire JA, Bayani J, Hide T, Henkelman RM, Cusimano MD, Dirks PB (2004) Identification of human brain tumour initiating cells. Nature.432(7015):396-401.
47. Soong R, Iacopetta BJ (1997) A rapid and nonisotopic method for the screening and sequencing of p53 gene mutations in formalin-fixed, paraffin-embedded tumors. Mod Pathol.10(3):252-8.
48. Stupp R, Hegi ME, Mason WP, van den Bent MJ, Taphoorn MJ, Janzer RC, Ludwin SK, Allgeier A, Fisher B, Belanger K, Hau P, Brandes AA, Gijtenbeek J, Marosi C, Vecht CJ, Mokhtari K, Wesseling P, Villa S, Eisenhauer E, Gorlia T, Weller M, Lacombe D, Cairncross JG, Mirimanoff RO (2009) Effects of radiotherapy with concomitant and adjuvant temozolomide versus radiotherapy alone on survival in glioblastoma in a randomised phase III study: 5-year analysis of the EORTC-NCIC trial. Lancet Oncol.10(5):459-66.
49. Suh H, Deng W, Gage FH (2009) Signaling in adult neurogenesis. Annu Rev Cell Dev Biol.25:253-75.
50. Tsai RY, McKay RD (2000) Cell contact regulates fate choice by cortical stem cells. J Neurosci.20(10):3725-35.
51. Visvader JE, Lindeman GJ (2012) Cancer stem cells: current status and evolving complexities. Cell Stem Cell.10(6):717-28.
52. Wen XZ, Akiyama Y, Baylin SB, Yuasa Y (2006) Frequent epigenetic silencing of the bone morphogenetic protein 2 gene through methylation in gastric carcinomas. Oncogene.25(18):2666-73.
53. Westphal M, Lamszus K (2011) The neurobiology of gliomas: from cell biology to the development of therapeutic approaches. Nat Rev Neurosci.12(9):495-508.
54. Wilson SI, Graziano E, Harland R, Jessell TM, Edlund T (2000) An early requirement for FGF signalling in the acquisition of neural cell fate in the chick embryo. Curr Biol.10(8):421-9.
55. Yan K, Wu Q, Yan DH, Lee CH, Rahim N, Tritschler I, DeVecchio J, Kalady MF, Hjelmeland AB, Rich JN (2014) Glioma cancer stem cells secrete Gremlin1 to promote their maintenance within the tumor hierarchy. Genes Dev.28(10):1085-100.
56. Youssef KK, Van Keymeulen A, Lapouge G, Beck B, Michaux C, Achouri Y, Sotiropoulou PA, Blanpain C (2010) Identification of the cell lineage at the origin of basal cell carcinoma. Nat Cell Biol.12(3):299-305.

Table 1. Basic demographic and clinical characteristics of patients

Patient	GSC-ECL	Sex	Age	Tumor site (Lobe)
2	G02	Female	61	Parietal
3	G03	Male	52	Temporal
5	G05	Male	52	Temporal
7	G07	Female	72	Temporal
8	G08	Female	62	Occipital
9	G09	Female	59	Frontotemporal

Table 2. Genetic and epigenetic alterations in brain tumors and in their respective GSC-ELCs.

SAMPLE	LOH 10q	LOH 1p	LOH 19q	*CDKN2A/ ARF* Deletion	*EGFR* Amplification	*EGFR vIII*	*TP53* Mutation	*MGMT* Gene Promoter Methylation	*IDH1* Mutation
G02 (Biopsy)	LOH	ROH	ROH	+	+ (x3)	-	-	+	-
G02 (GSC-ECL)	LOH	ROH	ROH	+	+ (x3)	-	-	+	-
G03 (Biopsy)	LOH	Partial LOH	ROH	+	+ (x55)	-	-	-	-
G03 (GSC-ECL)	LOH	Partial LOH	ROH	+	+ (x4)	-	-	-	-
G05 (Biopsy)	LOH	ROH	ROH	+	+ (x128)	+	-	-	-
G05 (GSC-ECL)	LOH	ROH	ROH	+	+ (x44)	+	-	-	-
G07 (Biopsy)	LOH	ROH	ROH	+	+ (x82)	-	-	-	-
G07 (GSC-ECL)	LOH	ROH	ROH	+	+ (x4)	-	-	-	-
G08 (Biopsy)	LOH	LOH	Partial LOH	+	+ (x244)	-	-	+	-
G08 (GSC-ECL)	LOH	LOH	Partial LOH	+	+ (x20)	-	-	+	-
G09 (Biopsy)	LOH	Partial LOH	ROH	-	-	-	+ (R248W)	-	-
G09 (GSC-ECL)	LOH	Partial LOH	ROH	+	-	-	+ (R248W)	-	-

EGFR amplification: estimated number of gene copies is indicated between brackets. LOH: Loss of heterozigosity; ROH: Retention of heterozigosity

Table 3. Cellular morphology and lineage marker expression of GSC-ECLs exposed to distinct experimental conditions.

GSC-ECL	+GF	-GF	-GF + BMP4 (0,5 ng/ml)	-GF + BMP4 (10 ng/ml)
G02	Homogeneous appearance with fusiform cells. $GFAP^+$ cells: - $MAP2^+$ cells: -	Heterogeneous appearance without a prevailing morphology. $GFAP^+$ cells: + $MAP2^+$ cells: +	Heterogeneous appearance without a prevailing morphology. $GFAP^+$ cells: + $MAP2^+$ cells: +	Heterogeneous appearance without a prevailing morphology. $GFAP^+$ cells: + $MAP2^+$ cells: +
G03	Homogeneous appearance with phase-dark cells. $GFAP^+$ cells: + $MAP2^+$ cells: -	Homogeneous appearance with flat cells. $GFAP^+$ cells: + $MAP2^+$ cells: -	Homogeneous appearance with flat cells. $GFAP^+$ cells: ++ $MAP2^+$ cells: -	Homogeneous appearance with flat cells. $GFAP^+$ cells: +++ $MAP2^+$ cells: -
G05	$GFAP^+$ cells displaying thin and long processes: +++ $MAP2^+$ neuronal-like cells: -	$GFAP^+$ astrocyte-like cells: ++ $MAP2^+$ neuronal-like cells: +	$GFAP^+$ astrocyte-like cells: ++ $MAP2^+$ neuronal-like cells: +	$GFAP^+$ astrocyte-like cells: +++ $MAP2^+$ neuronal-like cells: -
G07	Majority of cells displaying small cellular bodies with thin processes. $GFAP^+$ cells: - $MAP2^+$ cells: +	$GFAP^+$ cells with big cytoplasm: - $MAP2^+$ cells displaying small cellular bodies with thin processes: +++	$GFAP^+$ cells with big cytoplasm: + $MAP2^+$ cells displaying small cellular bodies with thin processes: ++	$GFAP^+$ astrocyte-like cells: +++ $MAP2^+$ neuronal-like cells: -
G08	Three sub-populations in similar proportions ($GFAP^+$ large cells, $MAP2^+$ tiny cells and double positive cells with variable morphology).	$GFAP^+$ astrocyte-like cells: ++ $MAP2^+$ neuronal-like cells: +	$GFAP^+$ astrocyte-like cells: +++ $MAP2^+$ neuronal-like cells: -	Flat $GFAP^+$ cells: +++ $MAP2^+$ cells: -
G09	Large $GFAP^+$ cells: - Small $MAP2^+$ cells: +++	$GFAP^+$ astrocyte-like cells: ++ $MAP2^+$ neuronal-like cells: ++	$GFAP^+$ astrocyte-like cells: +++ $MAP2^+$ neuronal-like cells: -	Flat $GFAP^+$ cells: +++ $MAP2^+$ cells: -

–: very low or undetectable percentages; +: low percentages; ++: high percentages: +++: very high percentages. GF: Growth factors

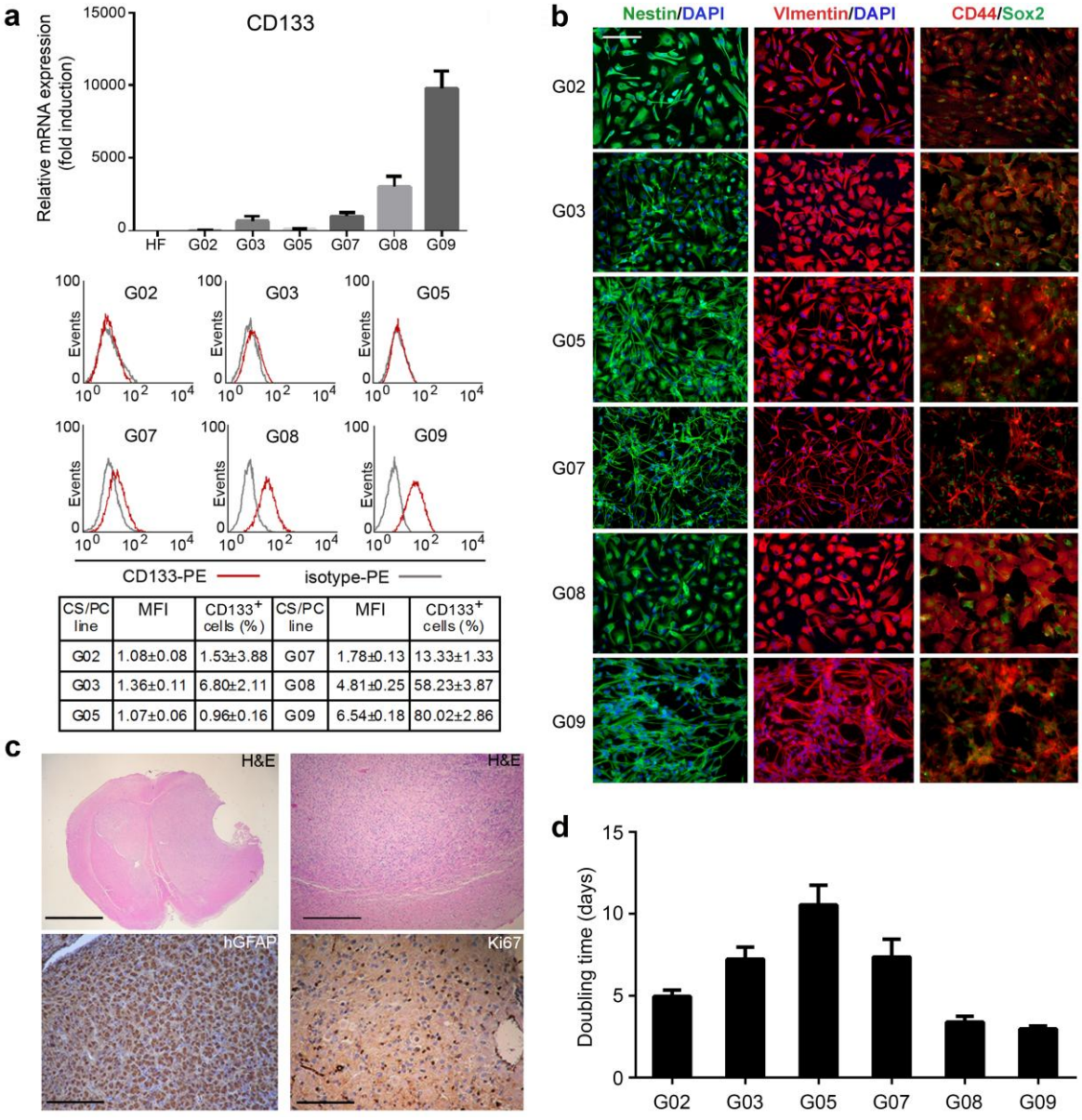

CS/PC line	MFI	CD133+ cells (%)	CS/PC line	MFI	CD133+ cells (%)
G02	1.08±0.08	1.53±3.88	G07	1.78±0.13	13.33±1.33
G03	1.36±0.11	6.80±2.11	G08	4.81±0.25	58.23±3.87
G05	1.07±0.06	0.96±0.16	G09	6.54±0.18	80.02±2.86

BPA_12263_F1

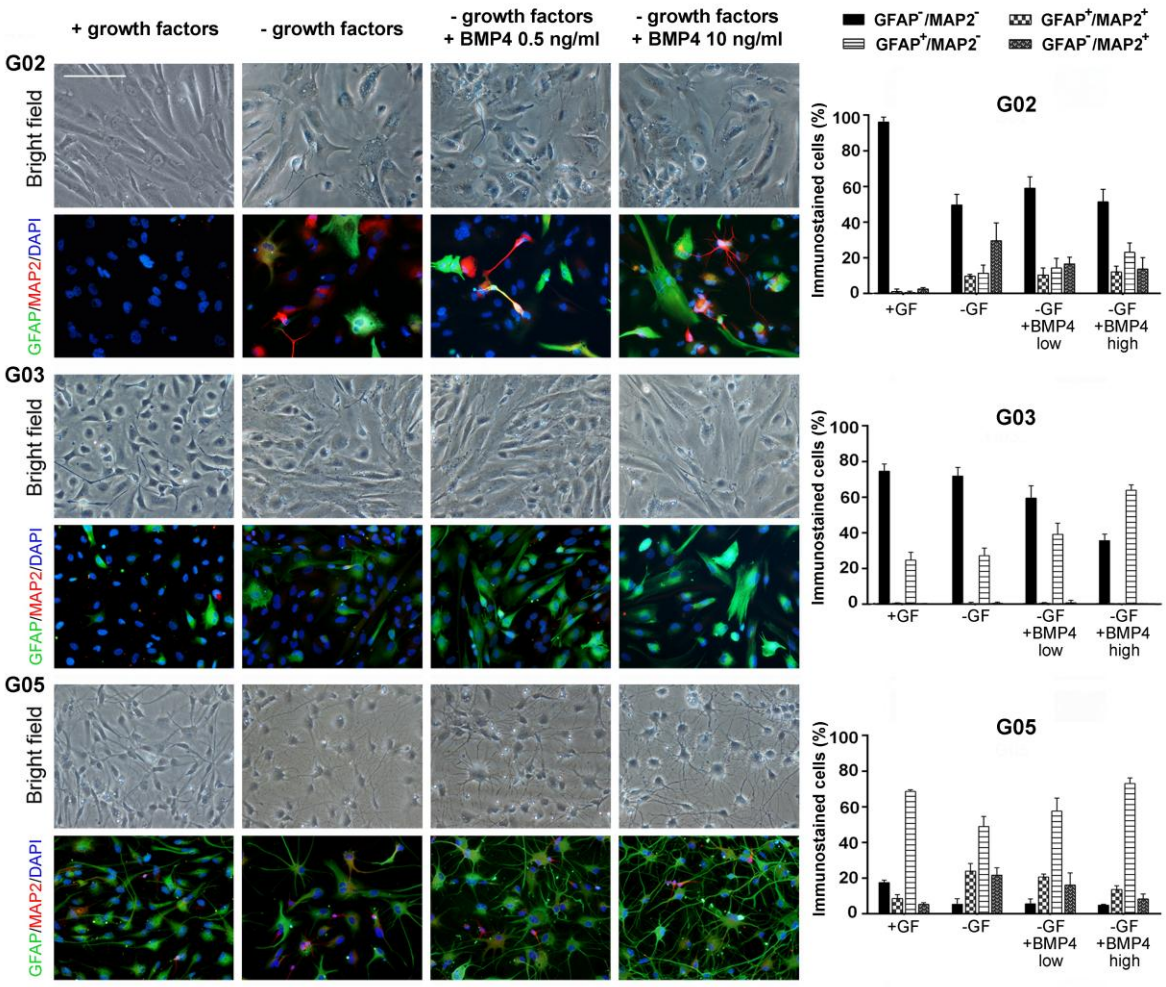

BPA_12263_F2

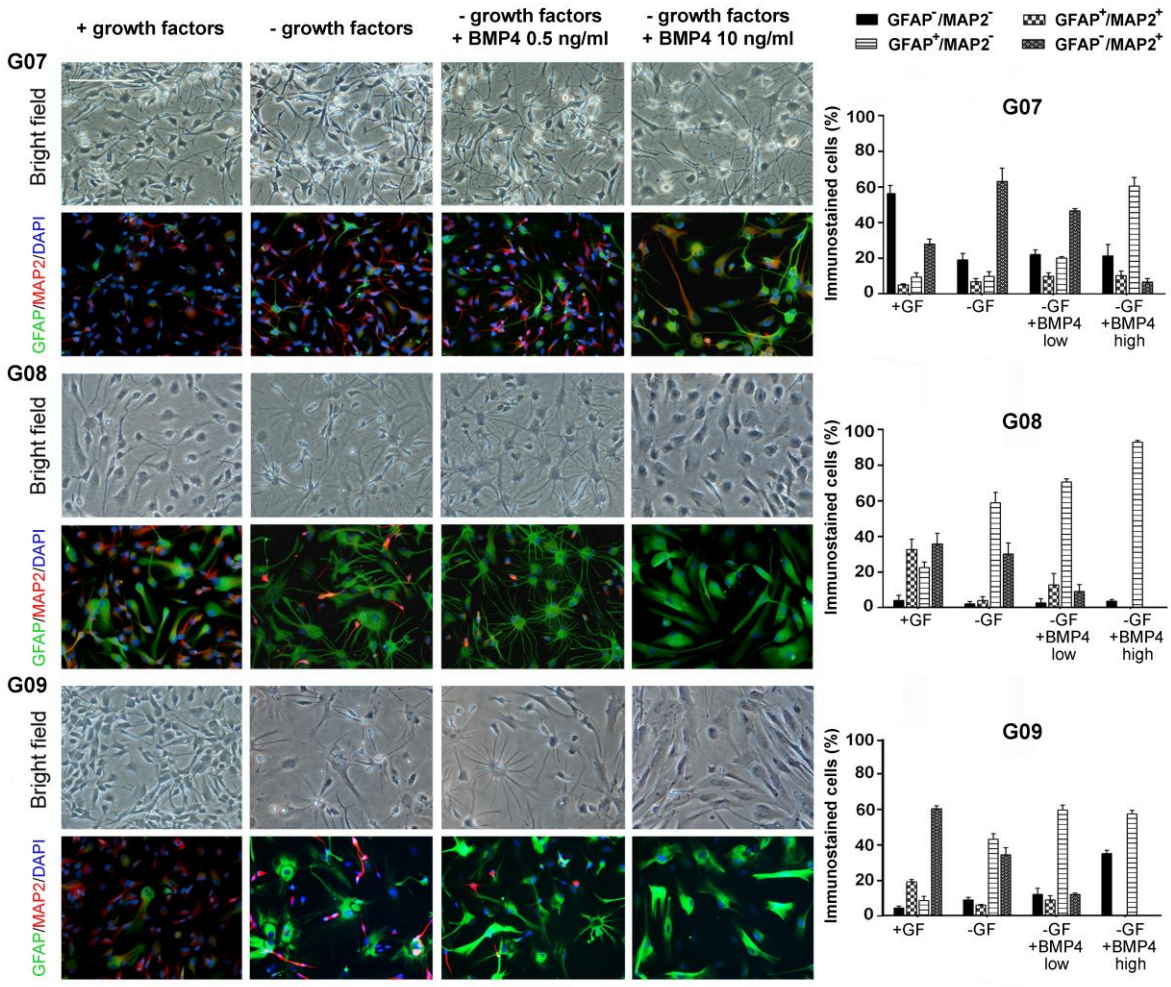

BPA_12263_F3

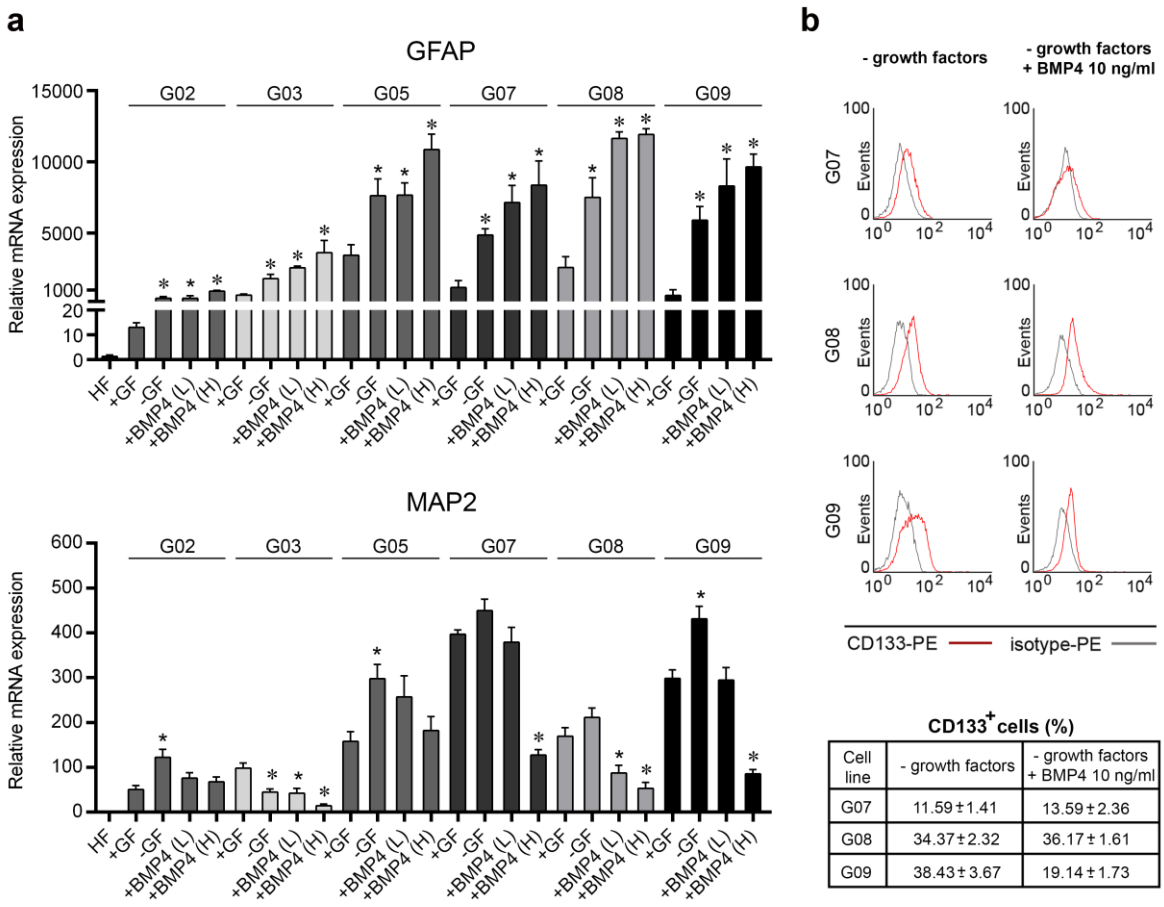

BPA_12263_F4

CD133$^+$ cells (%)

Cell line	- growth factors	- growth factors + BMP4 10 ng/ml
G07	11.59 ± 1.41	13.59 ± 2.36
G08	34.37 ± 2.32	36.17 ± 1.61
G09	38.43 ± 3.67	19.14 ± 1.73

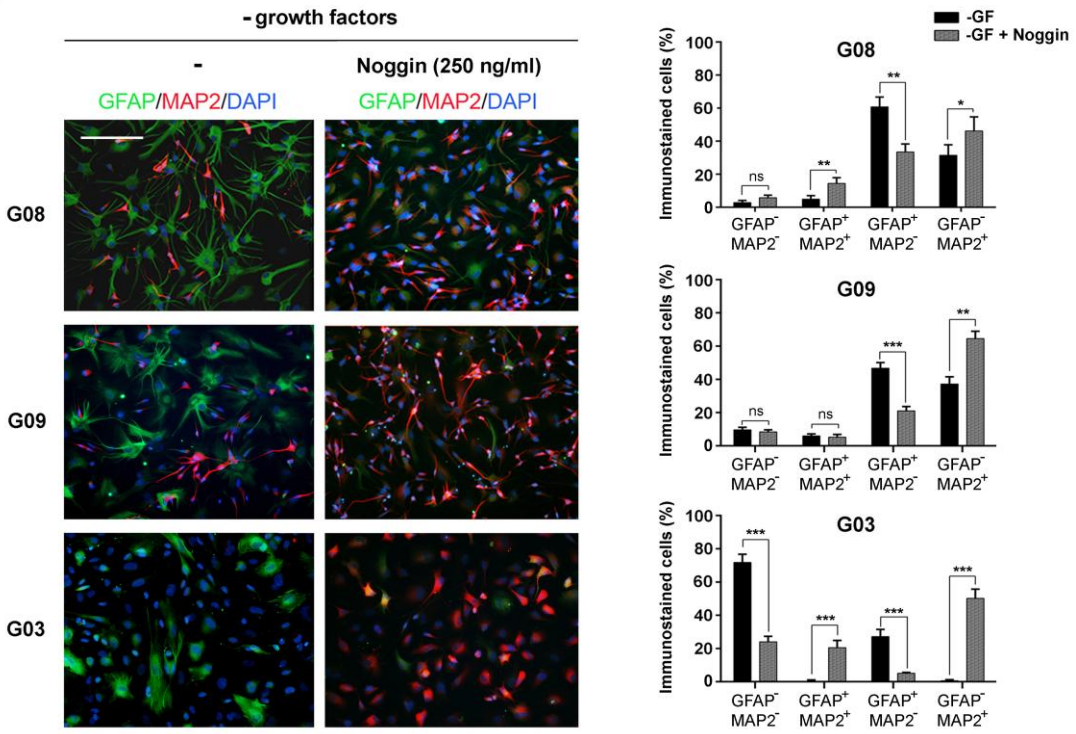

BPA_12263_F5

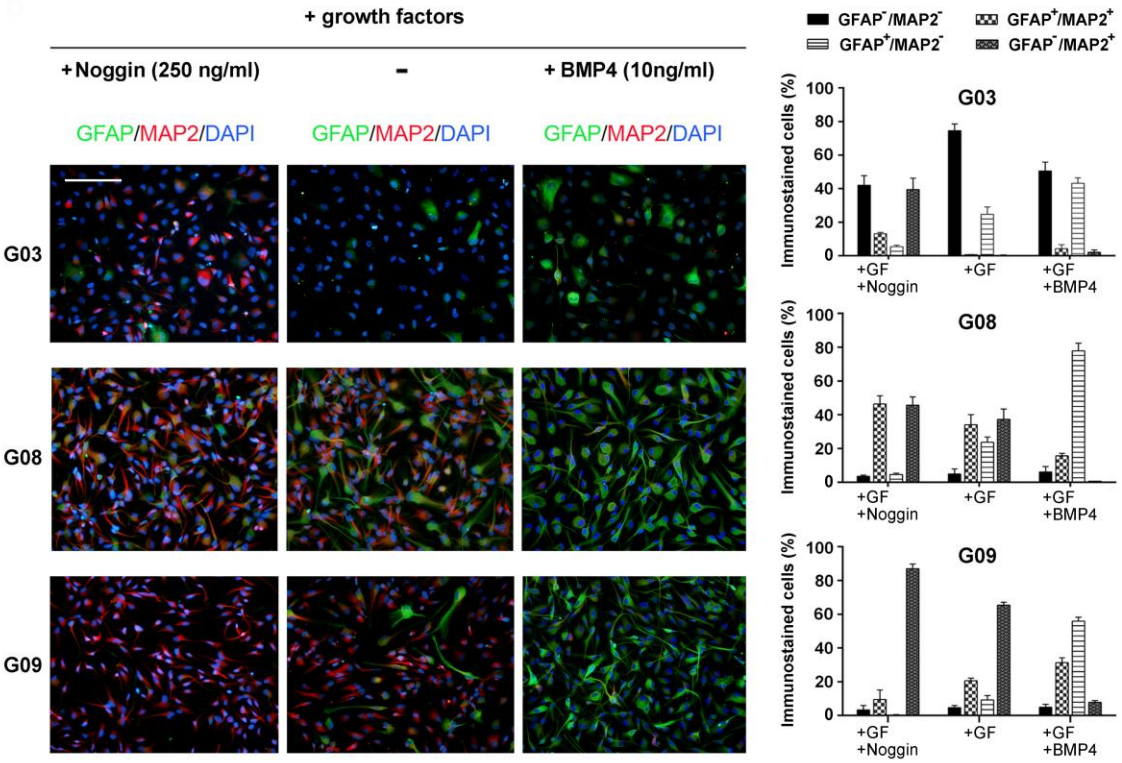

BPA_12263_F6

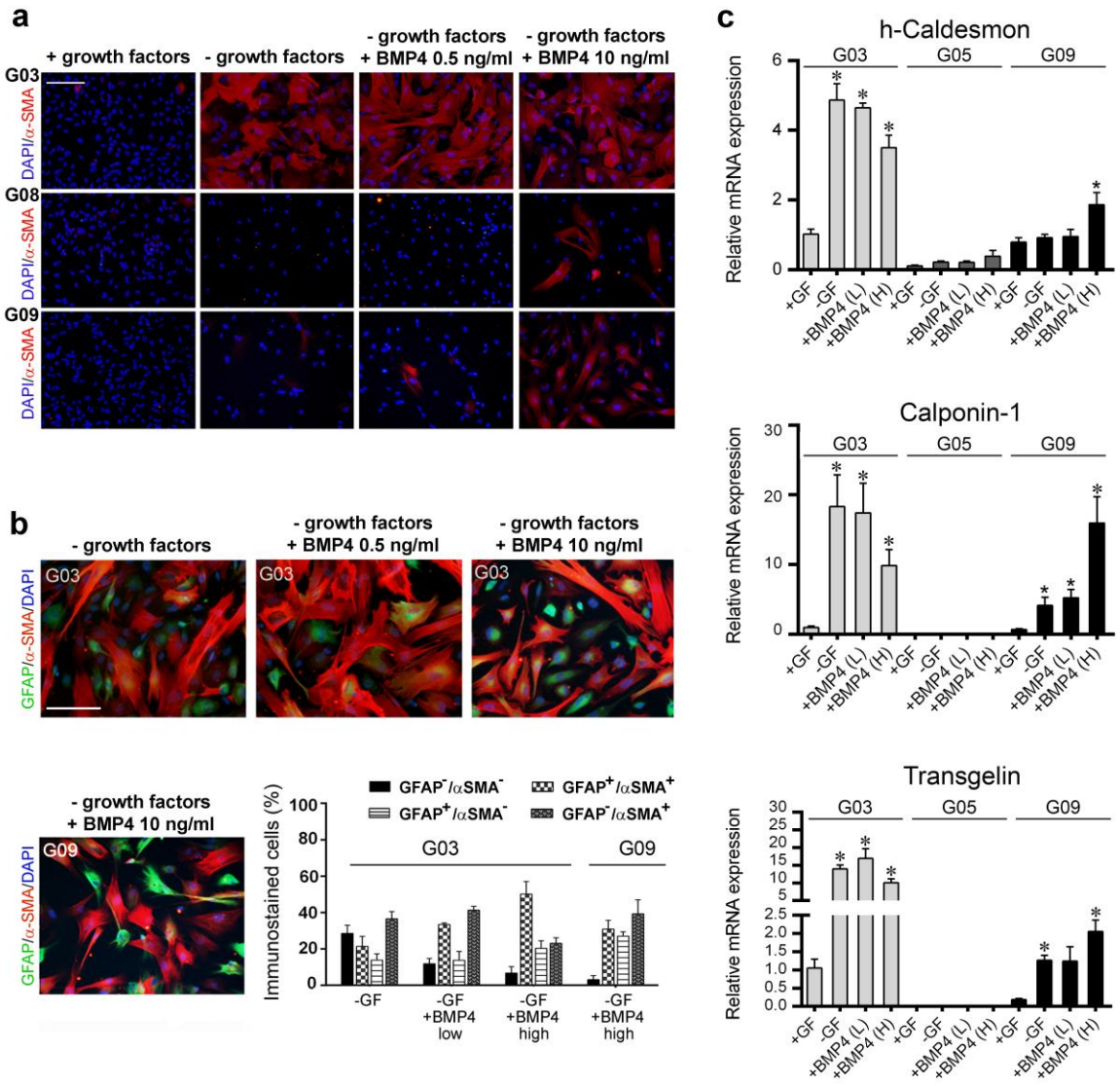

BPA_12263_F7

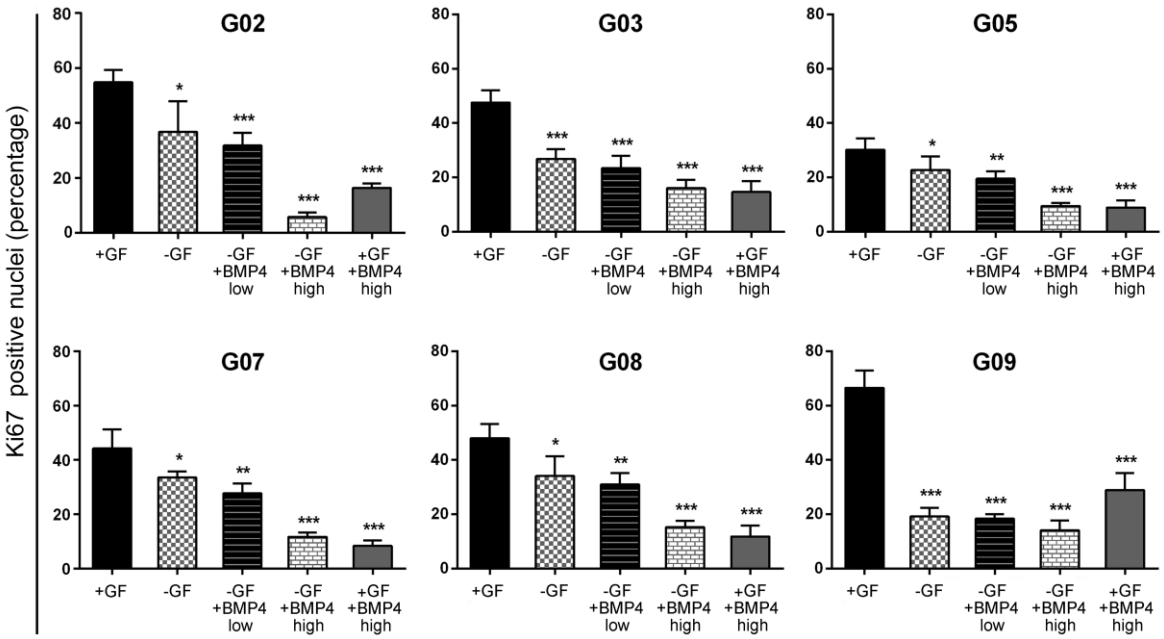

BPA_12263_F8

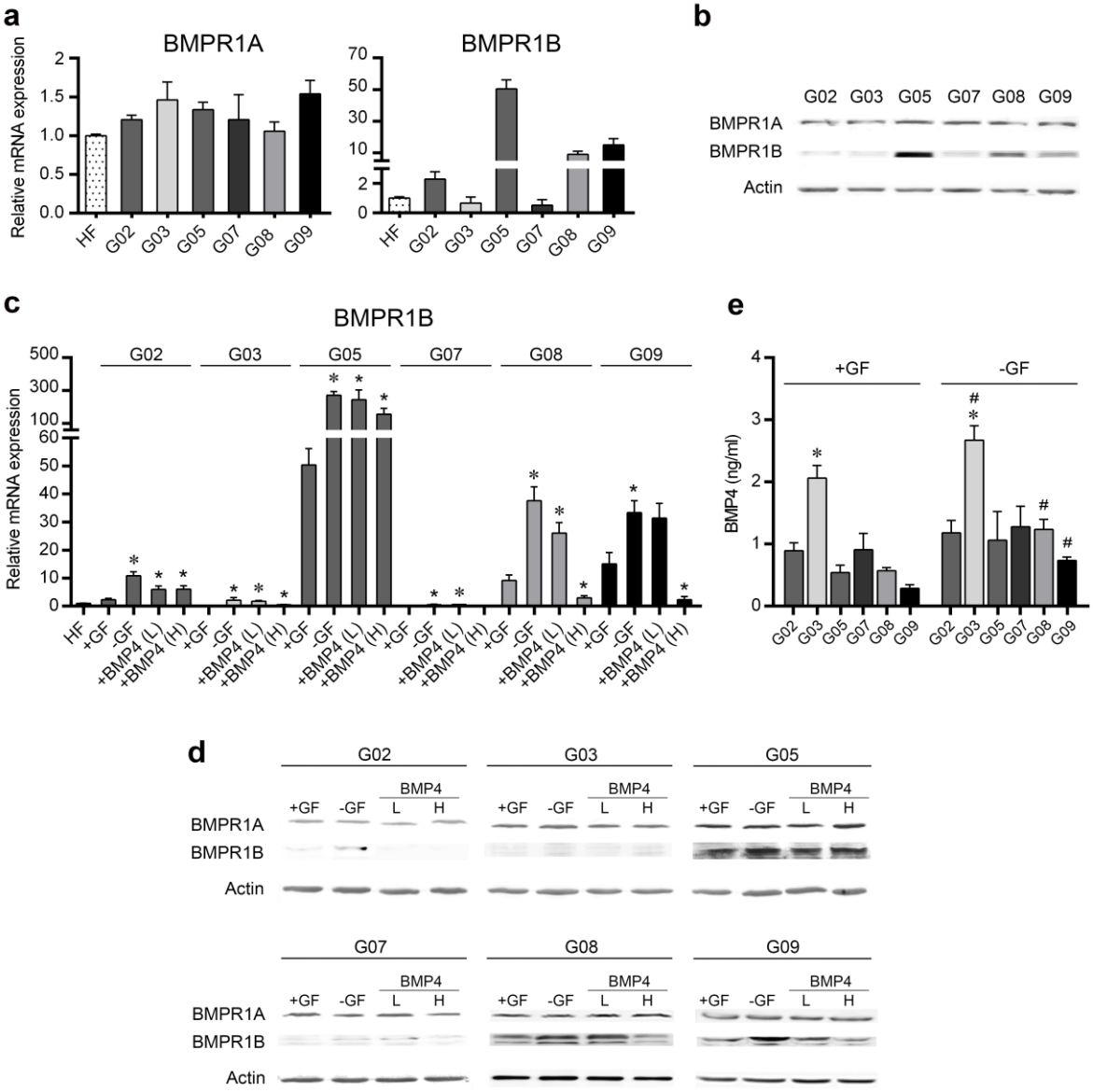

BPA_12263_F9